Supplementary Information for:

Retroviral promoters in the human genome

Andrew B. Conley, Jittima Piriyapongsa and I. King Jordan
School of Biology, Georgia Institute of Technology, 310 Ferst Drive, Atlanta, GA, 30306

Supplementary Methods

Paired end ditags (PETs)

Gene identification signature (GIS) analysis is a sequencing and mapping strategy that allows for the high-throughput demarcation of gene transcription boundaries, *i.e.* the 5' and 3' gene termini (Ng, et al., 2005). The GIS analysis procedure that produced the data we analyzed started with the isolation of polyA+ RNA from cells lines subject to different treatments: 1) the log phase of MCF7 cells, 2) MCF7 cells treated with estrogen (10nM beta-estradiol) for 12 hours, 3) HCT116 cells treated with 5FU (5-fluorouracil) for 6 hours, 4) the log phase of embryonic stem cell hES3 in feeder free culture condition. Full-length cDNAs (flcDNA) were generated from RNA and selected using the biotynlated CAP trapper method (Carninci, et al., 1996). The CAP trapper method relies on the introduction of a biotin group to the cap structure found at the 5' end of full length mRNAs followed by first strand cDNA synthesis. Biotin residues are selected using streptavidin-coated magnetic beads, which results in the retention of only flcDNAs. BamHI and MmeI restriction sites are ligated to the 5' and 3' termini of the flcDNAs, which are then cloned to produce the GIS-flcDNA library. This library is digested with MmeI to yielding 18bp sequence fragments (signatures) from the 5' and 3' ends of flcDNAs. The 3' end of the signature includes two A residues from the polyA tail. The 5' and 3' flcDNA signatures are covalently ligated to form 36bp paired-end ditags (PETs), each of which represents an individual transcript. PETs are exised using BamHI digestion and then concatenated and cloned for high-throughput sequencing. A single sequencing read of ~700bp leads, on average, to the characterization of 15 distinct PETs.

The GIS cloning and sequence analysis resulted in 584,624 PETs for the log phase MCF7 cells, 153,179 PETs for the estrogen-treated MCF7 cells, 280,340 PETs for the HCT116 cells, and 1,799,970 PETs for the hES3 cells. These PETs were then mapped to the human genome using the following criteria: paired 5' and 3' ends must be on the same chromosome, they must be in the correct 5'-to-3' order and orientation, they must be within 1 million base pairs, there must be a 16bp contiguous sequence match (out of 18bp) for the 5' end of the PET and a 14bp contiguous match (out of 16bp) for the 3' end of the PET. Using these criteria, most of the PET sequences (>90%) mapped to single locations in the human genome, but PETs mapping to 2-10 locations were also included in the analysis.

The quality and mapping specificity of PETs has been confirmed in a number of different ways (Ng, et al., 2005). For instance, >95% of PETs map to known human gene transcripts and the vast majority fell within 10bp of the transcription start and termination sites. Most relevant to our study is the fact that the GIS analysis has been shown to be 30 times more efficient than standard cDNA methods for characterizing transcript and has resulted in the discovery of numerous previously uncharacterized transcripts. Thus, GIS is particularly suited to the discovery of alternative transcripts in the human genome of the kind initiated by ERV sequences.

Cap Analysis of Gene Expression (CAGE)

The CAGE technique was developed for the high-throughput characterization of transcription start sites (TSS) (Shiraki, et al., 2003). CAGE uses a similar technology to that described above

for the generation of PETs in GIS. The main difference is that CAGE only characterizes the 5' ends, as opposed to both 5' and 3' PET ends, of flcDNAs. CAGE also employs the isolation of flcDNAs using biotinylated mRNA caps as described for GIS. Once flcDNAs are isolated, linkers with MmeI restriction sites are ligated to the 5' ends of the flcDNAs, and the first 20 bp of the cDNAs is cleaved with a MmeI restriction digest. The resulting 5' end cDNA fragments (so-called CAGE tags) are amplified, concatenated and sequenced. This procedure allows for the high-throughput characterization of the 5' ends of mRNAs, and mapping of the resulting sequence fragments to the genome identifies transcriptional start sites (TSS). CAGE tags are mapped to the human genome mandating a contiguous match of 18 out of 20bp. Approximately 60% of CAGE tags can be unambiguously mapped to the genome in this way. Only CAGE tags that mapped to one location in the genome were used in our study.

CAGE is a slightly more mature technology than GIS and it has been extensively validated (Carninci, et al., 2006; Kodzius, et al., 2006). In addition to the ability of CAGE tags to converge on known TSS in the human genome, CAGE also identifies thousands of previously unknown TSS. This is consistent with our discovery that numerous ERV-derived TSS correspond to alternative transcripts.

Gene expression analysis

Human and mouse gene expression data were taken from the Novartis mammalian gene expression atlas version 2 (GNF2) (Su, et al., 2004). GNF2 data are based on Affymetrix microarray experiments conducted in replicate on 79 human and 61 mouse tissues. For each Affymetrix probe, signal intensity values (*i.e.* expression levels) were median and log2 normalized across tissues. Affymetrix probes were mapped to GenBank RefSeq gene accessions using the UCSC Table Browser utility (Karolchik, et al., 2004). Human-mouse orthologous gene pairs and 28 corresponding tissue pairs were identified as described previously (Jordan, et al., 2004). Similarity between human-mouse orthologous gene pair tissue-specific expression profiles was measured using the Pearson correlation co-efficient (r) as described previously (Jordan, et al., 2005). An adjusted r-value threshold of 0.5789, above which human-mouse orthologous gene pairs can be considered to have correlated expression patterns across n=28 tissues, was computed using the formula $t=r*\mathrm{sqrt}((n-2)/(1-r^2))$, where t follows the Student-t distribution with n-2 degrees of freedom. The r-value threshold was based on a P-value of 0.00125 computed using a Bonferroni correction with the number of comparisons (40) performed (*i.e.* P=0.05/40).

The GNF2 data were also used to compare the values of a number of gene expression parameters for human genes that have ERV-TSS that yield chimeric transcripts (ERV+) versus all other human genes (ERV-) with Novartis expression data. Average values for the following gene expression parameters across the two sets were compared: 1) average expression, 2) maximum expression, 3) breadth of expression and 4) tissue-specificity of expression. Average, maximum and breadth of expression were computed as described previously in (Jordan, et al., 2005). Tissue-specificity was computed using the τ parameter described in (Yanai, et al., 2005). The values of τ range between 0 and 1 with more tissue-specific genes having higher values. Human gene tissue-specific expression profiles from the GNF2 data were used to group genes into 20 clusters of co-expressed genes with K-means clustering using the program Genesis (Sturn, et al., 2002). The observed counts of ERV+ genes in each of these clusters were compared to the expected counts based on the whole genome distribution using a chi-square test.

Human ESTs were mapped to ERV-derived TSS and associated genes and the tissues (or cell lines) from which they were characterized were determined using the Human ESTs track of the UCSC Genome Browser (Karolchik, et al., 2003). The distribution of EST tissue types across alternative versus primary promoters was compared using a joint chi-square test. Observed EST tissues counts for the alternative versus the primary TSS were compared with expected counts based on the pooled tissue counts to compute a chi-square value for each promoter and the joint chi-square probability for the two promoters was computed.

Gene ontology (GO) analysis

The set of human genes with ERV-TSS that yield chimeric ERV-gene transcripts (ERV+) were evaluated for enrichment of biological process and molecular function GO terms using the program using the program GOTree Machine (GOTM) (Zhang, et al., 2004). The GOTM program was used to implement a hypergeometric test comparing GO term frequencies in the ERV+ human gene set against a background set made up of all human genes with corresponding Affymetrix probes. GOTM produces a list of enriched GO terms along with a view of the GO directed acyclic graph (DAG) showing the parent-child relationships among enriched GO terms.

ERV age analysis

ERVs accumulate mutations after inserting into the genome. Thus, the relative ages of ERVs, *i.e.* the time since insertion, can be estimated using the sequence divergence levels between ERVs and their consensus sequences (Lander, et al., 2001). ERV-to-consensus divergence levels were taken from the RepeatMasker output. Average levels of ERV-to-consensus divergence were compared for all ERVs, ERVs that overlap with ESTs, ERVs that overlap with CAGE tags and ERVs that overlap with PETs.

Supplementary Results

Supplementary Table 1. **List of ERVs that inititate ERV-gene chimeric transcripts along with their associated genes.** Human genome location coordinates and names (accessions) are provided for the ERV and the gene. The locations of the ERVs relative to the RefSeq gene models are shown on the left: upstream, 5' UTR, In CDS.

	Name	Chromosome	Start	Stop	Gene Accession	Chromosome	Start	Stop
Upstream	LTR41	chr1	17954613	17954613	NM_030812	chr1	17954430	18026143
	MER4A	chr10	106004209	106004209	NM_004832	chr10	106004667	106017199
	LTR12D	chr14	23175701	23175701	NM_005794	chr14	23175421	23184686
	LTR12D	chr14	23175701	23175701	NM_182908	chr14	23175421	23184686
	MER54B	chr16	751307	751307	NM_005823	chr16	751133	758866
	MER54B	chr16	751307	751307	NM_013404	chr16	751133	758866
	MER39	chr17	7392869	7392869	NM_003809	chr17	7393098	7401930
	MER39	chr17	7392869	7392869	NM_172089	chr17	7393139	7405649
	MLT2E	chr19	9112101	9112101	NM_020933	chr19	9112072	9135082
	LTR12B	chr3	129354764	129354764	NM_021937	chr3	129355002	129610178
	LTR54	chr4	84425703	84425703	NM_015697	chr4	84404001	84424988
	MER41D-int	chr4	191144734	191144734	NM_020040	chr4	191140672	191143018
	MER51A	chr7	10979661	10979661	NM_014660	chr7	10980040	11109807
	MER51A	chr7	10979661	10979661	NM_001007157	chr7	10980040	11175766
	LTR43	chr8	143778578	143778578	NM_017527	chr8	143778532	143782611
	LTR75_1	chr8	144192262	144192262	NM_173687	chr8	144192053	144207095
In 5'-UTR	LTR41	chr1	17954234	17954613	NM_030812	chr1	17954430	18026143
	LTR41	chr1	17958237	17958696	NM_030812	chr1	17954430	18026143
	HERVH48	chr1	181939402	181944093	NM_015149	chr1	181871830	182164288
	HERV4_I	chr11	117598355	117598585	NM_001098526	chr11	117569651	117601019
	HERVL40	chr12	31766377	31766997	NM_207337	chr12	31715338	31773251
	LTR40a	chr13	29764513	29764758	NM_001014380	chr13	29674767	29779163
	LTR40a	chr13	29764513	29764758	NM_032116	chr13	29674767	29779584
	LTR12D	chr14	23176754	23177445	NM_005794	chr14	23175421	23184686
	LTR12D	chr14	23176754	23177445	NM_182908	chr14	23175421	23184686
	MLT2E	chr19	9111991	9112101	NM_020933	chr19	9112072	9135082
	MER67D	chr19	42033104	42033171	NM_003419	chr19	42033106	42062310
	MER52D	chr2	109729279	109729386	NM_023016	chr2	109729199	109733852
	Harlequin	chr2	188083923	188088834	NM_001032281	chr2	188051551	188127464
	LTR16C	chr20	4666836	4667196	NM_177549	chr20	4659928	4669314
	LTR7	chr4	89292502	89292904	NM_004827	chr4	89230440	89299035
	LTR1D	chr4	178965922	178966704	NM_001085490	chr4	178886900	179148663
	HERV9	chr5	146361399	146364490	NM_181674	chr5	145949260	146415783
	HERV9	chr5	146361399	146364490	NM_181678	chr5	145949260	146441207

	LTR5B	chr5	177414929	177415182	NM_001080544	chr5	177414995	177415888
	LTR50	chr8	12873949	12874595	NM_020844	chr8	12847553	12931655
	LTR43	chr8	143778243	143778578	NM_017527	chr8	143778532	143782611
	HERVH	chrX	113744197	113747503	NM_000868	chrX	113724806	114050880
	LTR41	chrX	134693953	134694178	NM_152582	chrX	134693879	134701914
	LTR41	chrX	134693953	134694178	NM_001017436	chrX	134693879	134719184
	LTR41	chrX	134781361	134781586	NM_001007551	chrX	134773630	134781660
	LTR41	chrX	134798611	134798836	NM_001017438	chrX	134790881	134798910
In CDS	MER54B	chr16	725416	725902	NM_022493	chr16	719771	730998
	LTR9	chrX	2729224	2729740	NM_175569	chrX	2680114	2743960
	MER51A	chr2	3339561	3340106	NM_003310	chr2	3171749	3360605
	MER21C	chr7	5933542	5933818	NM_001099697	chr7	5932302	5976840
	MER21C	chr7	5933542	5933818	NM_173565	chr7	5932302	5976840
	MER31B	chr8	11702728	11703173	NM_004462	chr8	11697598	11734226
	LTR36	chr22	17028682	17028800	NM_017414	chr22	17012757	17040162
	MER41A-int	chr12	26797075	26797151	NM_002223	chr12	26379553	26877398
	LTR12	chr12	29480709	29481473	NM_183378	chr12	29471755	29541886
	HERVE	chr12	31165336	31165939	NM_001080502	chr12	31158726	31250355
	LTR27B	chr7	33358011	33358250	NM_001033604	chr7	33135676	33612205
	LTR27B	chr7	33358011	33358250	NM_001033605	chr7	33135676	33612205
	LTR27B	chr7	33358011	33358250	NM_014451	chr7	33135676	33612205
	LTR27B	chr7	33358011	33358250	NM_198428	chr7	33135676	33612205
	MLT2B2	chr17	34767819	34768179	NM_032875	chr17	34670366	34811402
	MER41G	chr22	34984494	34985070	NM_003661	chr22	34979069	34993522
	MER41G	chr22	34984494	34985070	NM_145343	chr22	34979069	34993522
	LTR7	chr18	38577764	38578263	NM_002930	chr18	38577189	38949655
	MER68	chr4	38951204	38951750	NM_025132	chr4	38860418	38963824
	LTR19C	chr13	42526886	42527709	NM_013238	chr13	42495361	42581304
	MER61F-int	chr15	43131729	43132168	NM_003104	chr15	43102632	43154331
	MER92C	chr4	46920855	46921054	NM_000812	chr4	46728335	47123202
	LTR12C	chr13	50224579	50226004	NM_198989	chr13	50184759	50315886
	MER4C-int	chr7	50525903	50526498	NM_000790	chr7	50493627	50596262
	MER4C-int	chr7	50525903	50526498	NM_001082971	chr7	50493627	50600648
	MER4D	chr3	54650117	54651004	NM_018398	chr3	54131732	55083622
	MER21C	chr5	54816203	54816867	NM_003711	chr5	54756441	54866630
	MER21C	chr5	54816203	54816867	NM_176895	chr5	54756441	54866630
	MER34B	chr4	62321975	62322273	NM_015236	chr4	62045433	62620762
	HERV4_I	chr19	63452392	63453769	NM_014480	chr19	63431881	63466820
	MER57A-int	chr6	64070948	64072854	NM_016571	chr6	64047518	64087841
	MER52A	chr4	64888385	64889631	NM_001010874	chr4	64826015	64957773
	LTR12	chr7	68888991	68889595	NM_015570	chr7	68702254	69895790

	MER52A	chr13	69395827	69397313	NM_020866	chr13	69172726	69580460
	MER4B-int	chr12	74045504	74047192	NM_152779	chr12	74014729	74050436
	MER34B	chr9	74532752	74533337	NM_138691	chr9	74326536	74641087
	MLT2F	chr7	75145897	75146022	NM_005338	chr7	75001344	75206215
	MLT2B2	chr12	79840894	79841339	NM_004664	chr12	79715301	79855825
	HERV17	chr8	81814505	81817335	NM_001033723	chr8	81713323	81949571
	LTR54	chr1	85637738	85638265	NM_012137	chr1	85556756	85703411
	HERVH	chr10	92557476	92561145	NM_000872	chr10	92490557	92607651
	HERVH	chr10	92557476	92561145	NM_019859	chr10	92490557	92607651
	HERVH	chr10	92557476	92561145	NM_019860	chr10	92490557	92607651
	HERVH	chr4	93581454	93584375	NM_001510	chr4	93444572	94912672
	LTR9	chr7	98858058	98858575	NM_015545	chr7	98854689	98874355
	MER34D	chr13	99168644	99168812	NM_206808	chr13	99056936	99342824
	HERVH	chr14	101779943	101781050	NM_014226	chr14	101764930	101841284
	MLT2D	chr7	110096425	110096839	NM_032549	chr7	110090345	110989583
	LTR12C	chr4	110124142	110125521	NM_198721	chr4	109954420	110443248
	LTR12C	chr4	110124142	110125521	NM_032518	chr4	109964489	110443248
	HERVH	chr8	110382902	110385440	NM_032869	chr8	110322324	110415491
	LTR16C	chr12	116670959	116671316	NM_173598	chr12	116375221	116777724
	LTR22B	chr10	117136681	117136898	NM_207303	chr10	116843113	117698484
	LTR7Y	chr3	117306893	117307327	NM_002338	chr3	117011839	117647068
	HERVH	chr3	117309183	117312335	NM_002338	chr3	117011839	117647068
	LTR7Y	chr3	117312335	117312765	NM_002338	chr3	117011839	117647068
	LTR16B	chr9	118368734	118369128	NM_198188	chr9	118227327	118489334
	LTR16B	chr9	118368734	118369128	NM_014010	chr9	118227327	119217138
	LTR16B	chr9	118368734	118369128	NM_198186	chr9	118227327	119217138
	LTR16B	chr9	118368734	118369128	NM_198187	chr9	118227327	119217138
	HUERS-P3	chr6	119008185	119016806	NM_001042475	chr6	118892931	119079713
	HUERS-P3	chr6	119008185	119016806	NM_206921	chr6	118919289	119079713
	MER41B	chr8	119012088	119012717	NM_000127	chr8	118880782	119193239
	MLT2B4	chr8	119444631	119445182	NM_001101676	chr8	119270875	119703365
	LTR38B	chr6	119666263	119666850	NM_005907	chr6	119540967	119712625
	LTR12C	chr3	120273950	120275501	NM_152538	chr3	120102170	120347588
	LTR7	chr6	123945179	123945578	NM_006073	chr6	123579181	123999641
	MER52A	chr4	124247306	124248778	NM_145207	chr4	124063674	124460054
	MER21A	chr6	124675036	124675939	NM_001040214	chr6	124166767	125188483
	LTR22C	chr7	126086080	126086529	NM_000845	chr7	125865892	126670546
	LTR40a	chr8	126207807	126207882	NM_173685	chr8	126173276	126448543
	MLT2A2	chr3	126756469	126756970	NM_022776	chr3	126730393	126796624
	LTR10C	chr5	133976397	133976985	NM_001033503	chr5	133970018	133996426
	LTR10C	chr5	133976397	133976985	NM_016103	chr5	133970018	133996426

	PABL_A	chr9	135137645	135138270	NM_020469	chr9	135120383	135140451
	MER21C	chr2	137646118	137646928	NM_001080427	chr2	137464931	138151757
	HERV9	chr5	146361399	146364490	NM_181676	chr5	145949260	146415671
	HERV9	chr5	146361399	146364490	NM_181677	chr5	145949260	146441207
	LTR1B	chr7	146429315	146430028	NM_014141	chr7	145444385	147749019
	LTR8A	chr7	147352928	147353621	NM_014141	chr7	145444385	147749019
	MER21A-int	chr4	147875445	147878401	NM_031956	chr4	147847628	148086484
	MER4A1-int	chr3	151891622	151892158	NM_152394	chr3	151860366	151904432
	HERV30	chr3	155568283	155571737	NM_001038705	chr3	155538155	155630198
	MER41B	chr6	160579903	160580541	NM_003058	chr6	160557783	160599949
	HUERS-P2	chr3	168448261	168451231	NM_024687	chr3	168440778	168580765
	LTR10G	chr3	168474996	168475504	NM_024687	chr3	168440778	168580765
	LTR7	chr4	187400103	187400470	NM_000892	chr4	187385665	187416618
	HERVH	chr4	187402139	187405364	NM_000892	chr4	187385665	187416618
	HERVL40	chr2	202090151	202090443	NM_152525	chr2	202060401	202192146
	MER21C	chr1	223825852	223826508	NM_001008493	chr1	223741156	223907468
	MER21C	chr1	223825852	223826508	NM_018212	chr1	223741156	223907468
	LTR49-int	chr2	231087179	231087883	NM_003113	chr2	230989114	231089486
	LTR49-int	chr2	231087179	231087883	NM_001080391	chr2	230989114	231118561

Supplementary Figure 1. **ERV-derived promoter of the LY6K gene.** A) The LTR43 (red) ERV sequence is located in the proximal promoter region and overlaps the LY6K 5' UTR. The locations of PET sequences (green) and spliced ESTs (black) are shown. B) The LTR43 (red) sequence region is enlarged and the individual PET sequences (green) and spliced ESTs (black) that support the existence of this promoter are shown. C) Evolutionary conservation of LY6K versus LY6K.

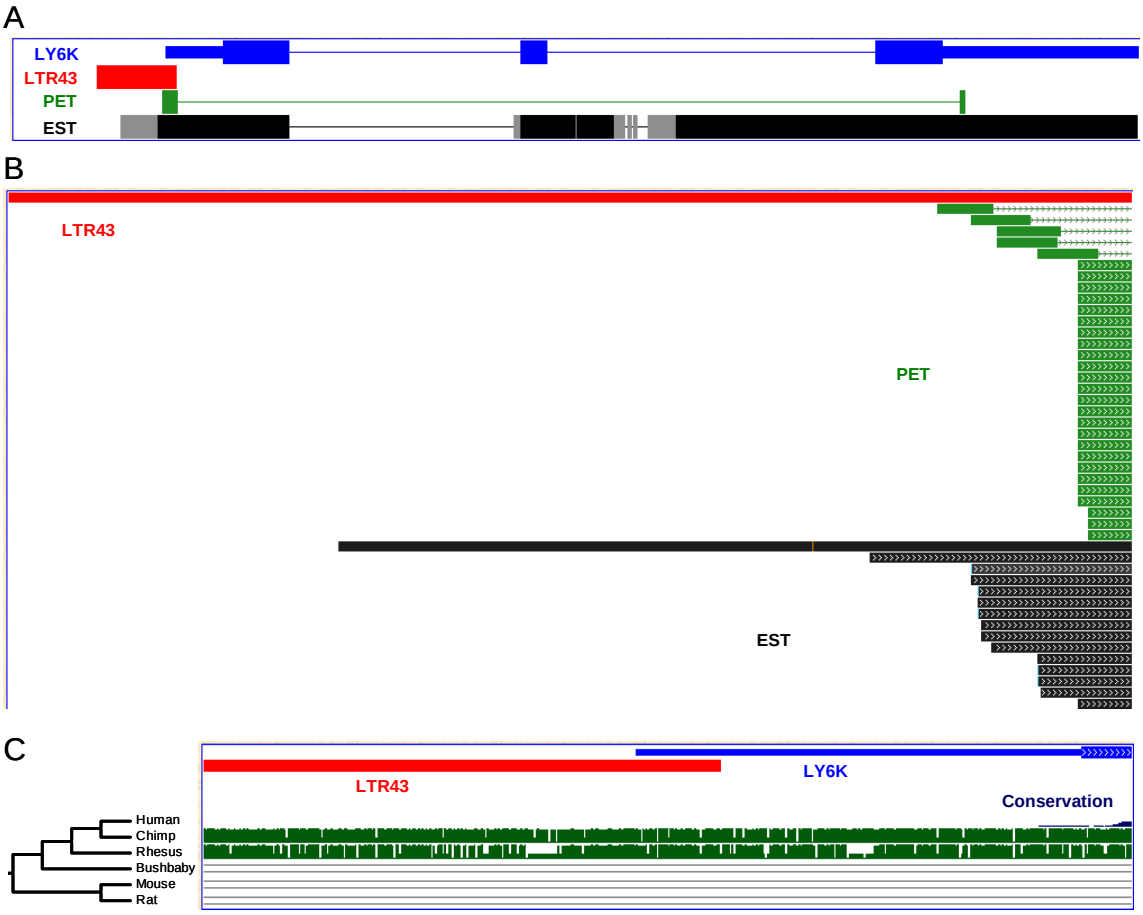

Supplementary Figure 2. **Gene expression profiles and correlations for human and mouse *GSTO1* and *GSTO2*.** A) Relative expression values resulting from median and log2 normalization of Affymetrix signal intensity values across tissues. B) Pearson correlation coefficient values (*r*) showing the correlation, or lack thereof, for tissue-specific expression between human paralogs and human-mouse orthologs.

A

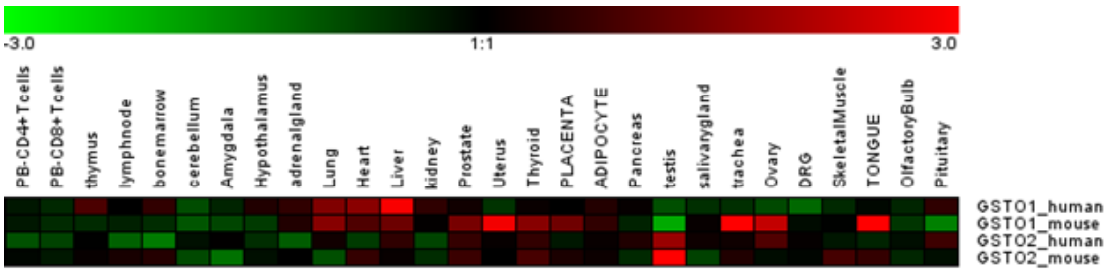

B

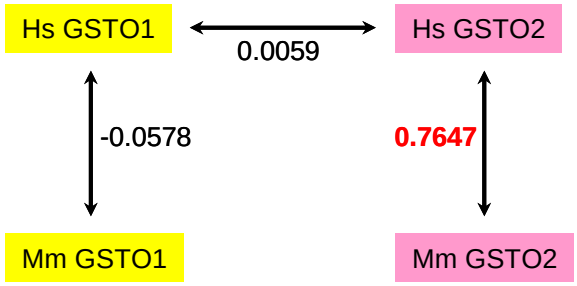

Supplementary Figure 3. **Ranked list of *r*-values showing the correlation between human-mouse orthologous gene tissue-specific expression profiles for all human genes that have a lineage-specific ERV-derived TSS that generates a chimeric ERV-gene transcript.** An *r*-value≥0.5789, dotted line, corresponds to significantly co-expressed orthologous gene pairs.

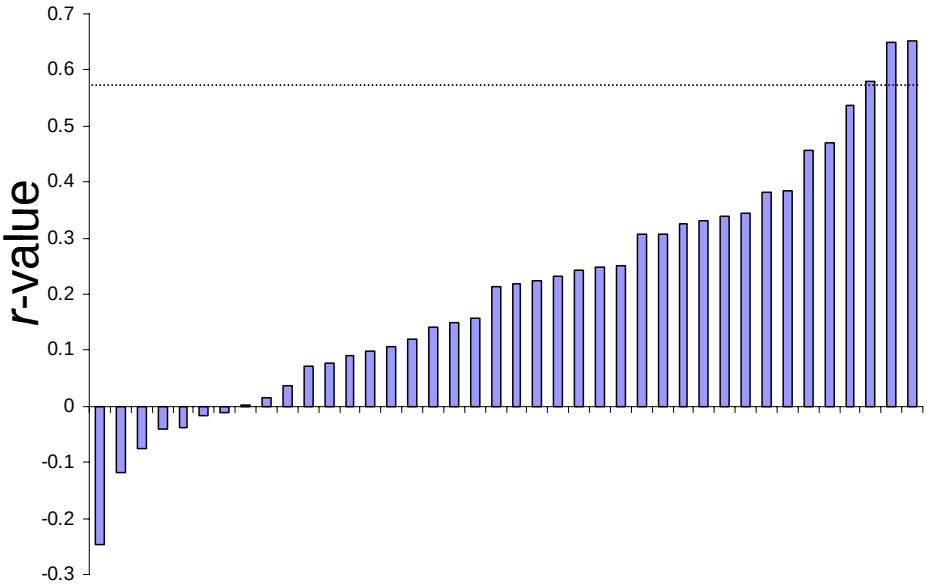

Supplementary Table 2. **Human gene expression values for genes with ERV-TSS versus all other genes.**

Expression[1]	**ERV+**[2]	**ERV-**[3]	***t***[4]	***P***[4]
Average	378.3 ± 52.9	600.6 ± 10.0	3.97	7.3e-5
Maximum	1920.1 ± 309.9	3143.5 ± 50.33	3.76	1.7e-4
Breadth	23.9 ± 2.6	27.0 ± 0.1	1.18	2.4e-1
Tissue-specificity	0.75 ± 0.01	0.71 ± 0.00	2.88	4.0e-3

[1]Expression parameters measured using the Novartis GNF2 data as described
[2]Average and standard error for human genes possessing an ERV that promotes an ERV-gene chimeric transcript
[3]Average and standard error for all other human genes
[4]Test statistic and significance level for the Student's *t*-test comparing the ERV+ and ERV- values

Supplementary Figure 4. **Co-expressed clusters of human genes.** Average tissue-specific expression profiles across 79 tissues are shown for each cluster. Clusters enriched for genes with ERV-TSS that generate chimeric transcripts are boxed in red. Chi-square statistical analysis indicating enrichment in cluster 1 (brain) and cluster 20 (testis) is shown below the clusters.

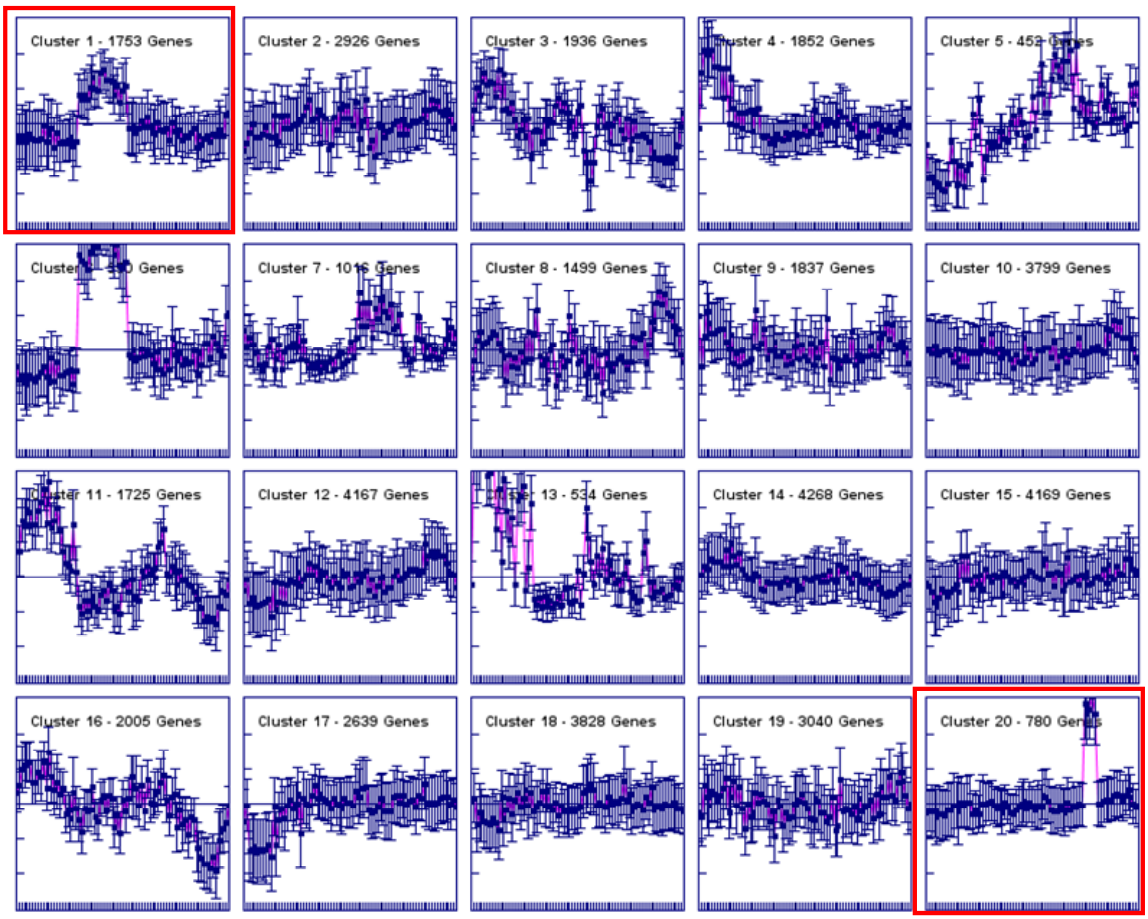

cluster	#probe	Observed	Expected	chi-square	
1	1753	12	3.87598	17.02787535	brain
2	2926	4	6.469548	0.9426727	
3	1936	1	4.280603	2.514214961	
4	1852	4	4.094874	0.00219815	
5	452	2	0.999397	1.001810501	
6	550	2	1.21608	0.5053366	
7	1016	4	2.246432	1.368837315	
8	1499	1	3.314372	1.616088155	
9	1837	3	4.061709	0.277524844	
10	3799	6	8.399799	0.685615837	
11	1725	1	3.81407	2.07625744	
12	4167	4	9.213467	2.950055682	
13	534	1	1.180704	0.02765619	
14	4268	7	9.436784	0.629230882	
15	4169	14	9.217889	2.480891257	
16	2005	7	4.433166	1.486215024	
17	2639	7	5.834975	0.23261172	
18	3828	5	8.46392	1.417633857	
19	3040	6	6.721608	0.077469284	
20	780	8	1.724623	22.83418023	testis
	44775	99		60.15437598	Chi-square value
				3.65815E-06	*P*-value

Supplementary Figure 5. **Human gene co-expression cluster 1 (brain) and cluster 20 (testis) are shown**. Average relative expression levels are indicated on the y-axis and the tissue-names are shown on the x-axis below the second panel.

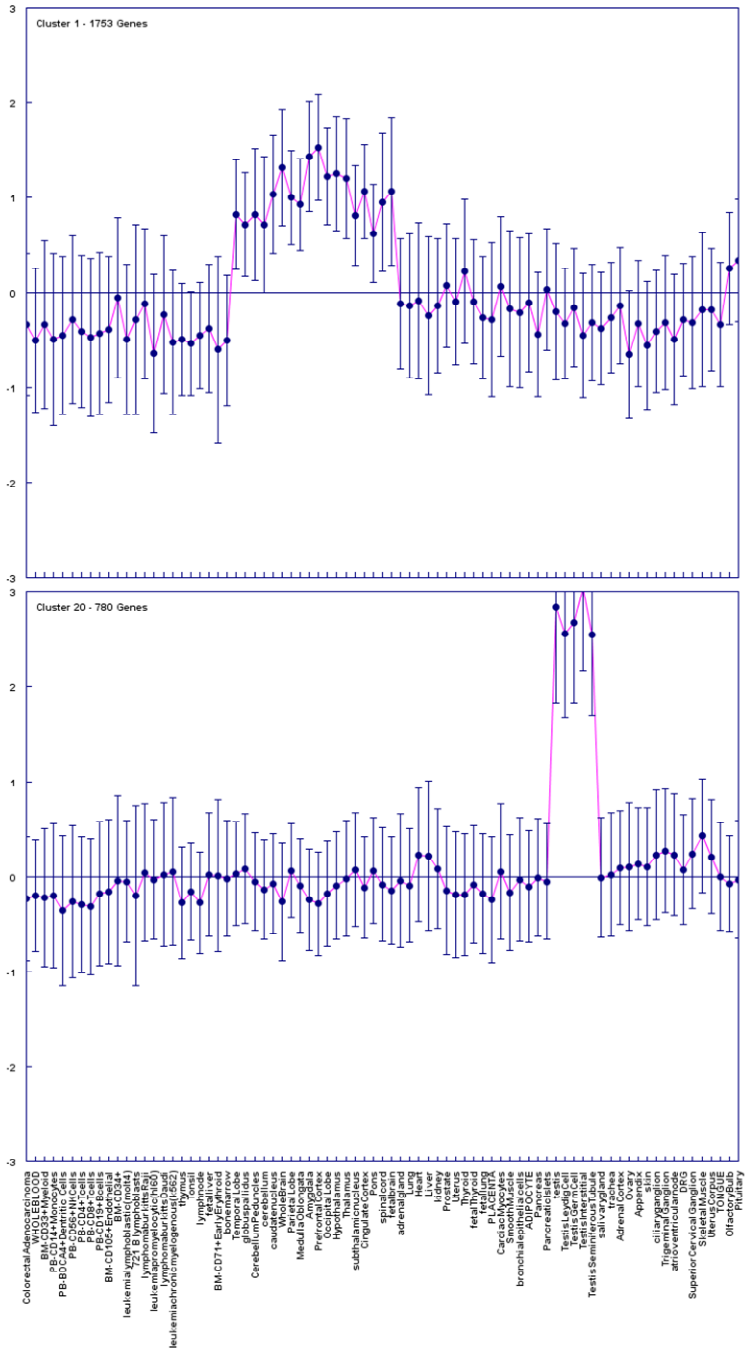

Supplementary Figure 6. **Tissue distribution of ERV CAGE tags.** Observed counts for ERV CAGE tags are compared to expected counts based on all CAGE tags for brain, testis and the average of all other tissues. χ^2=3,249 *P*=0.

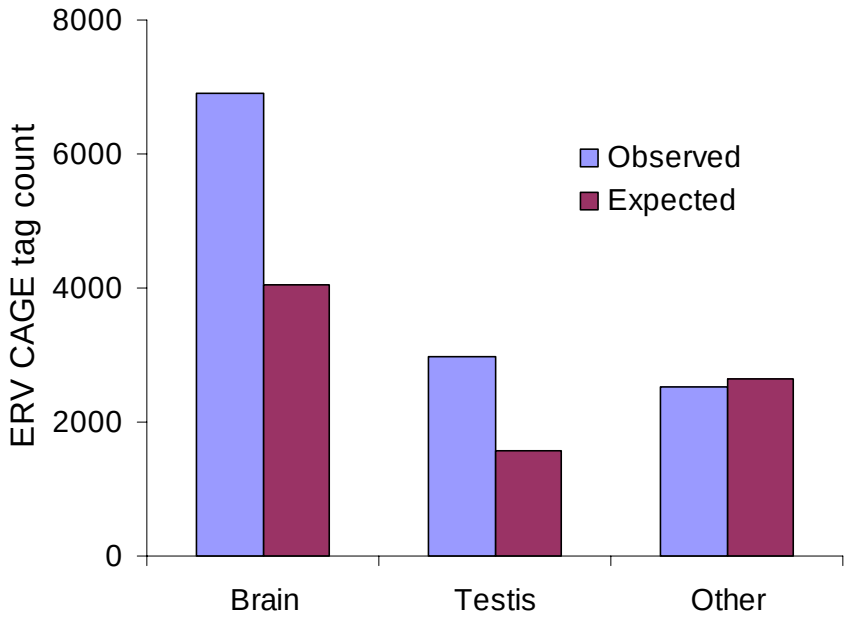

Supplementary Table 3. **Statistically over-represented (enriched) GO biological process terms for human genes with an ERV-derived TSS generating a chimeric ERV-gene transcript.**

AffyID[a]	ERV-gene[b]	GO[c]	*P*-value[d]
201563_at	NM_003104	GO:0019751 polyol metabolic process	0.0015
205311_at	NM_000790, NM_001082971	GO:0006066 alcohol metabolic process	0.0034
206463_s_at	NM_005794, NM_182908	GO:0008202 steroid metabolic process	0.0030
208647_at	NM_004462	GO:0008299 isoprenoid biosynthetic process	0.0013
209546_s_at	NM_003661, NM_145343	GO:0008202 steroid metabolic process	0.0030
210946_at	NM_003711, NM_176895	GO:0044255 cellular lipid metabolic process	0.0089
213379_at	NM_015697	GO:0008299 isoprenoid biosynthetic process	0.0013
218304_s_at	NM_022776	GO:0008202 steroid metabolic process	0.0030

[a]AffyID mapped to ERV-related gene
[b]ERV-related gene
[c]Over-represented biological process GO term and description
[d]*P*-value associated with that GO term

Supplementary Figure 7. **GO directed acyclic graph showing the parent-child relationships of statistically over-represented (enriched) GO biological process and molecular function terms for human genes with an ERV-derived TSS generating a chimeric ERV-gene transcript.** Significantly enriched GO terms are shown in red.

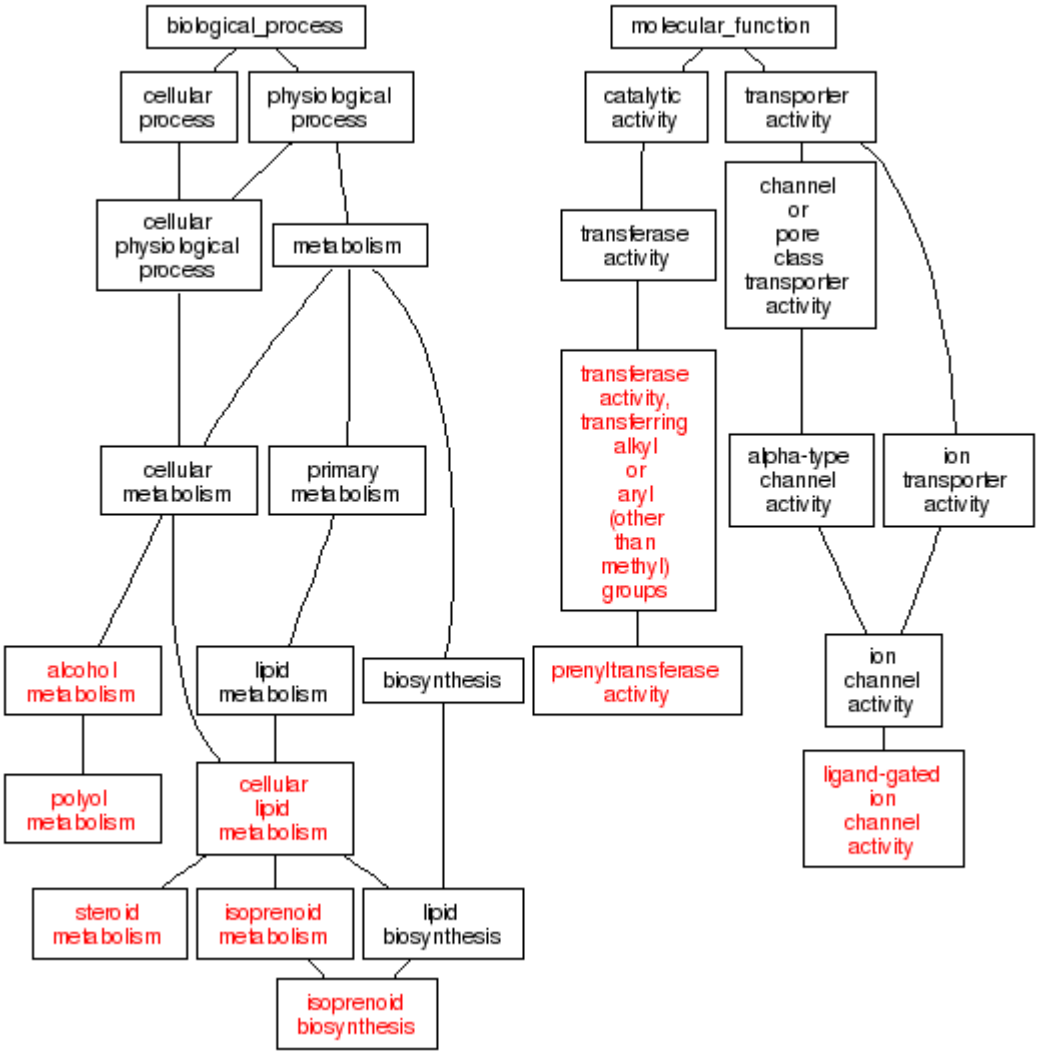

Supplementary Figure 8. **Relative frequency of ERV-derived TSS detected by PET versus all ERVs in the genome.** ERV types correspond to family names from the RepeatMasker output.

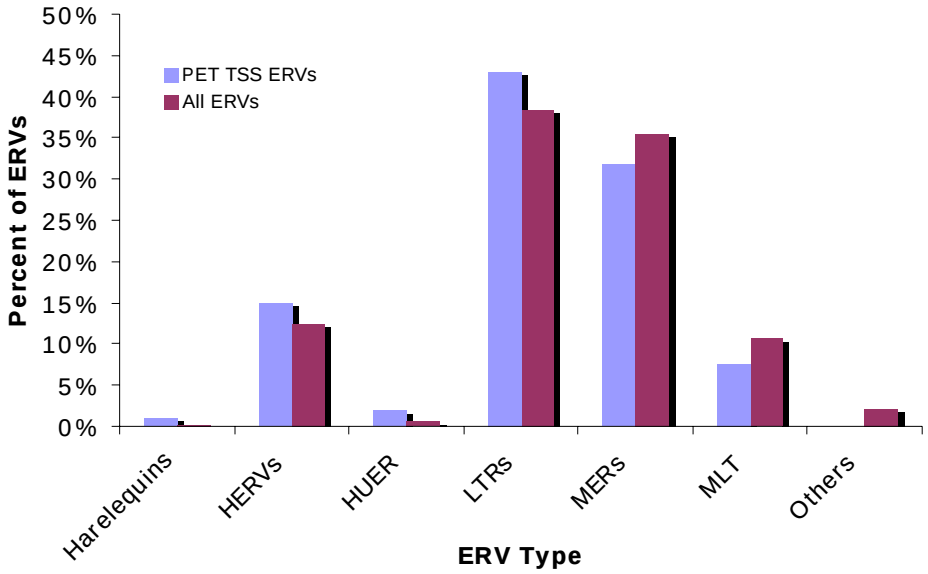

Supplementary Table 4. **Average percent divergence between ERVs and their consensus sequences.** Divergence is shown for all ERVs and for ERVs that overlap ESTs, CAGE tags and PET tags.

ERVs	% Divergence	Number
All ERVs	19.6 ± 0.01	322,408
EST ERVs	16.5 ± 0.15	2,678
CAGE ERVs	19.7 ± 0.04	39,559
PET ERVs	13.8 ± 0.16	2,249

Supplementary References

Carninci, P., et al. (1996) High-efficiency full-length cDNA cloning by biotinylated CAP trapper, *Genomics*, **37**, 327-336.

Carninci, P., et al. (2006) Genome-wide analysis of mammalian promoter architecture and evolution, *Nat Genet*, **38**, 626-635.

Jordan, I.K., et al. (2005) Evolutionary significance of gene expression divergence, *Gene*, **345**, 119-126.

Jordan, I.K., et al. (2004) Conservation and coevolution in the scale-free human gene coexpression network, *Mol Biol Evol*, **21**, 2058-2070.

Karolchik, D., et al. (2003) The UCSC Genome Browser Database, *Nucleic Acids Res*, **31**, 51-54.

Karolchik, D., et al. (2004) The UCSC Table Browser data retrieval tool, *Nucleic Acids Res*, **32**, D493-496.

Kodzius, R., et al. (2006) CAGE: cap analysis of gene expression, *Nat Methods*, **3**, 211-222.

Lander, E.S., et al. (2001) Initial sequencing and analysis of the human genome, *Nature*, **409**, 860-921.

Ng, P., et al. (2005) Gene identification signature (GIS) analysis for transcriptome characterization and genome annotation, *Nat Methods*, **2**, 105-111.

Shiraki, T., et al. (2003) Cap analysis gene expression for high-throughput analysis of transcriptional starting point and identification of promoter usage, *Proc Natl Acad Sci U S A*, **100**, 15776-15781.

Sturn, A., et al. (2002) Genesis: cluster analysis of microarray data, *Bioinformatics*, **18**, 207-208.

Su, A.I., et al. (2004) A gene atlas of the mouse and human protein-encoding transcriptomes, *Proc Natl Acad Sci U S A*, **101**, 6062-6067.

Yanai, I., et al. (2005) Genome-wide midrange transcription profiles reveal expression level relationships in human tissue specification, *Bioinformatics*, **21**, 650-659.

Zhang, B., et al. (2004) GOTree Machine (GOTM): a web-based platform for interpreting sets of interesting genes using Gene Ontology hierarchies, *BMC Bioinformatics*, **5**, 16.